



UNSTEADY BOUNDARY LAYER FLOW OF WILLIAMSON NANOFUIDS OVER A HEATED PERMEABLE STRETCHING SHEET EMBEDDED IN A POROUS MEDIUM IN THE PRESENCE OF VISCOUS DISSIPATION.

H. D. Hunegnaw¹

¹Department of Mathematics, Debre Markos University, Debre Markos, P.O. box 269, Ethiopia

Email: tewdroshunex@gmail.com

Abstract:

The main objective of this paper is to make investigation on a numerical study of unsteady boundary layer flow of Williamson Nanofluids over a heated permeable stretching sheet embedded in a porous medium in the presence of viscous dissipation. A mathematical model which resembles the physical flow problem has been developed. By using an appropriate transformation, I converted the system of dimensional nonlinear partial differential equations into a system of coupled dimensionless ordinary differential equations. Numerical solutions of these equations are obtained by Runge-Kutta fourth order with shooting method. The velocity, temperature and concentration distributions are discussed numerically and presented through graphs. The numerical values of reduced skin-friction coefficient, Nusselt number and Sherwood number at the plate are derived and discussed numerically for various values of physical parameters which are presented through tables. The present results have been compared with existing one for some limiting case and found excellent validation. It is analyzed that the reduced skin friction coefficient enhances with increasing values of an unsteady parameter, magnetic parameter and porosity parameter. In addition, it is observed that a decrease in the velocity profile of the fluid flow for increasing values of the non-Newtonian Williamson parameter and a rise in Eckert number leads to the enhancement of the temperature of the fluid in the thermal boundary layer.

Keywords: Porous medium, Williamson nanofluids, porous medium, MHD, viscous dissipation, fourth order Runge-Kutta method

1. Introduction

The theory of boundary layer flow was first introduced by the German scientist Prandtl in 1904. This flow refers to a kind of flow in a relatively narrow region near a solid surface where the effect of viscosity is significant. On the other hand, the study of fluid flow on a stretching surface is one of the important problems in the current area, as it occurs in different processes of engineering for example, extrusion, wire drawing, food manufacturing, metal spinning, manufacturing of rubber sheets and cooling of huge metallic plates such as an electrolyte, etc. The problem of boundary layer approximations over stretching surface was first introduced by Sakiadis (1961). Crane (1970) obtained the closed form solution for the flow investigated by the stretching of flexible parallel sheet moving periodically. Gupta and Gupta (1977) extended this work by considering suction/blowing at the surface of the sheet. Pop (1996) studied time-dependent flow over a stretched surface. Following these pioneer works, many investigators have reported various useful study results. For instance, the effect of linear thermal stratification in stable stationary on steady MHD convection flow of a viscous incompressible electrically conducting fluid along a stretching sheet in the presence of mass transfer and magnetic effect was analysed by Kumar (2013) using Fourth order Runge-Kutta method. Also, Narasa et.al (2016) used perturbation technique to obtain analytic solution for free convection unsteady fluid flow in the presence of thermal diffusion and chemical reaction past a vertical porous plate with heat source and slip effects.

Fluids that do not satisfy Newtonians law of viscosity are known as non-Newtonian fluids such as Blood, paints, Ketchup, shampoo, mud, etc. Williamson fluid is one of non-Newtonians fluids. Williamson fluid is characteristic of non-Newtonian fluid model with shear thinning property. It is one of those fluids that show both viscous and elastic properties, now called pseudo plastic fluids.

NOMECLATURE

(x, y)	Cartesian coordinates of a representative point	M	Magnetic parameter
(u, v)	Velocity components along x and y -axis	s	Suction/injection parameter
A_1	First-Erickson tensor	Ec	Eckert number
T_∞	Ambient temperature	Sc	Schmidt number
C_w	Wall concentration	Re_x	Local Reynolds number
C_∞	Ambient concentration	Rd	Thermal radiation parameter
C	Fluid concentration	MHD	Magnetohydrodynamic
c	Prop. constant of the velocity of the sheet		
T	Fluid temperature		Greek Symbol
S	Cauchy stress	α	Positive constant
Pr	Prandtl number	ρ	Fluid density
U_∞	Free stream velocity	ν	Kinematic viscosity
U_w	Wall velocity	η	Non-dimensional similarity variable
B_0	Initial Magnetic field	ψ	Stream function
c_p	Specific heat at constant pressure	μ	Dynamic Viscosity
k_r	Reaction rate of the fluid	β	Casson fluid parameter
c_f	Skin friction coefficient	θ	Dimensionless Fluid temperature
Nu_x	Nusselt number	φ	Dimensionless nanoparticle concentration
Sh_x	Sherwood number	γ	chemical reaction parameter
we	Weissenberg number		

Williamson (1929) discussed the flow of pseudo plastic materials and presented a model equation to discuss the pseudo plastic fluids flow and verified the results experimentally, and later on used by several variables authors (Dapra et al. (2007); Vasuadev et al. (2010), Nadeen et al. (2010); Nadeen et al. (2014, 2016) to investigate fluid flow by using optimal homotopy analysis method (OHAM) and perturbation method to solve the governing system of equation for Williamson fluid. Gossaye et al. (2019) optimal Homotopy Asmptotic solution for cross-Diffusion on slip flow and heat transfer of electrical MHD Non-Newtonian fluid over a slendeing stretching sheet. Analytic Treatment for Electrical MHD Non-Newtonian Fluid Flow over a Stretching Sheet through a Porous Medium was investigated by Gossaye (2020). Recently, flows of non-Newtonian fluids in the boundary layer have drawn considerable attention because of their significant applications in processing of metallurgical, phenomena of chemical engineering transport, molten polymers, extrusion, plastic sheets and wrapping toils fabrication, etc. Species, momentum and heat transport play major roles in such processes (1996). There are many applications of non-Newtonian fluids especially in the behaviour of pseudoplastic fluid which is widely applied in industrial applications. It is equally important in the biological engineering for example to measure the mass and heat transfer through the vessels in blood and hemodialysis (2017). Hence, many researchers [Khan et al. (2018), Mabood et al. (2017), Vijayalaxmi et al. (2016), Goud et al.(2020)] investigate this fluid flow with respect to various conditions.

Nanofluid is a mixture of continuous base fluid component called a matrix and a discontinuous solid component called nanoparticles (1–100 nm) which are used to enhance the thermal conductivity of the nanofluid. The nanoparticles are made of metals or metallic oxides. The novelty of nanofluids offer fascinating heat transfer characteristics compared to conventional heat transfer fluids. These particles are made up of metals such as (Al, Cu), oxides (Al_2O_3), carbides (SiC), nitrides (AlN, SiN) or nonmetals (Graphite, carbon nanotubes). Choi (1995) experimentally verified that addition of small amount of these particles in the base fluid results in the appreciable increase in the effective thermal conductivity of the base fluid such as water. Recently, researchers have used this concept of nanofluid as a route to enhance the performance of heat transfer rate in liquids. Although nanofluids have been studied almost completely as Newtonian fluid, very recently, their rheological properties have been established by the non-Newtonian model of nanofluid transport phenomena. Many studies have concentrated on non-Newtonian fluid as a base fluid with suspended nanoparticles over a stretching and moving sheet. Bilal Ashraf et al. (2015) studied the convective heat and mass transfer in MHD mixed convection flow of Jeffrey nanofluid over a radially stretching surface with thermal radiation. Shehzad et al. (2015) discussed the influence of thermophoresis and Brownian motion on the flow and heat transfer of incompressible third-grade nanofluid in the presence of Newtonian heating and viscous dissipation over a stretching sheet. Madhu et al. (2015) numerically investigated two-dimensional MHD mixed convection

boundary layer stagnation-point flow, heat, and mass transfer of a non-Newtonian Power-law nanofluid toward a stretching surface. The effects of radiation and chemical reaction on the steady boundary layer flow of MHD Williamson fluid through porous medium toward a horizontal linearly stretching sheet in the presence of nanoparticles were investigated numerically by Krishnamurthy et al. (2016). Kho et al. (2017) analyzed the boundary layer flow of Williamson nanofluids past over a stretching sheet in the presence of thermal radiation effect. Shawky et al. (2019) also examined the MHD flow with heat and mass transfer of Williamson nanofluids over stretching sheet through porous medium. Recently, Tesfaye et al. (2020) utilized the homotopy analysis method to investigate heat and mass transfer in unsteady boundary layer flow of Williamson nanofluids. Effect of viscous dissipation on MHD Williamson Nanofluid flow in a porous medium was investigated by Manjula et al. (2019). The Investigation of MHD Williamson Nanofluid over Stretching Cylinder with the Effect of Activation Energy was done by Ibrahim et al. (2020). However, to the best of the author’s knowledge, no study has been reported on the numerical solution of time dependent boundary layer flow of Williamson nanofluids over a permeable stretching sheet embedded in a porous medium with the effects of magnetic field, thermal radiation, chemical reaction and viscous dissipation using Fourth order Runge Kutta method along shooting technique. Thus, motivated by the aforementioned works, the present study attempts to fill the existing gaps in this area. Hence, the aim of the current research is to investigate the heat and mass transfer for MHD unsteady boundary layer flow of Williamson Nanofluids over a heated permeable stretching sheet embedded in porous medium in the presence of viscous dissipation. A numerical solution of this fluid flow problem is obtained by using the Runge-Kutta method in conjugation with the shooting technique. Numerical results of the Nusselt number, skin friction coefficient, and Sherwood number for different values of the physical parameters are computed in tables. The effects of different physical parameters on dimensionless velocity, temperature, and concentration are presented in graphs.

2. Mathematical Formulation of the Problem

Consider a two-dimensional unsteady boundary layer flow of an incompressible Williamson nanofluid over a permeable stretching sheet embedded in a porous medium. The sheet is stretched along the x -axis with velocity $u_w = \frac{ax}{1-ct}$, where a and c are positive constants with dimension $(time)^{-1}$ as shown below in Figure 1.

Assume the time-dependent magnetic field $B(t) = \frac{B_0}{\sqrt{1-ct}}$ is applied in the y -direction, where B_0 is the initial magnetic field strength and $ct < 1$. It is assumed that the induced magnetic field is negligible in comparison with the applied magnetic field. The fluid velocity, temperature and nanoparticle concentration near the surface are assumed to be U_w , T_w and C_w , respectively. The ambient fluid temperature and concentration are denoted by T_∞ and C_∞ respectively. Further, u and v are the velocity components in the direction of x and y , respectively.

Details of the Williamson fluid model can be found in Nadeem et al. (2013). For the present Williamson fluid model, Cauchy stress S is defined in Dapra et al. (2007) as

$$S = -PI + \tau, \tag{1}$$

where τ = extra stress tensor and is given by

$$\tau = \left(\mu_\infty + \frac{\mu_0 - \mu_\infty}{1 - \Gamma \xi} \right) A_1, \tag{2}$$

where μ_0 is limiting viscosity at zero shear rate; μ_∞ is limiting viscosity at the infinite shear rate; $\Gamma > 0$ is time constant; and A_1 is first Rivlin-Ericksen tensor.

Further, ξ is defined as

$$\xi = \sqrt{\frac{\Pi}{2}}, \quad \Pi = \text{Trace}(A_1^2). \tag{3}$$

Consider the case for which $\mu_\infty = 0, \Gamma \xi < 1$.

$$\text{Then} \quad \tau = \mu_0(1 - \Gamma \xi)A_1. \tag{4}$$

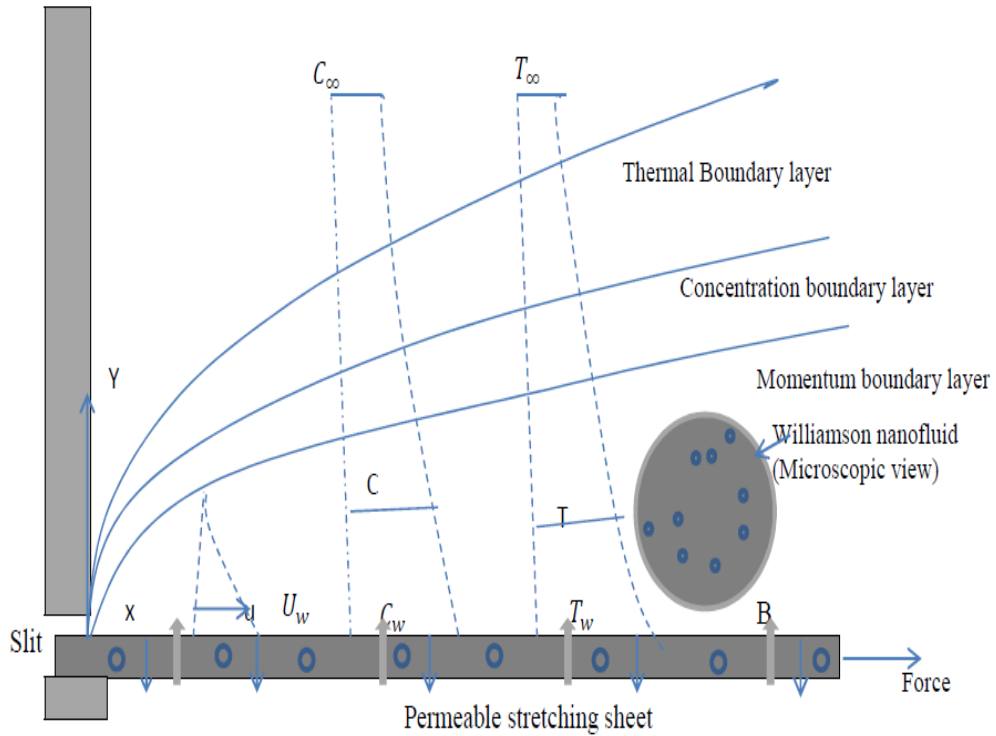


Fig. 1: Physical configuration of the flow model

Using the assumptions given above, the governing equations of continuity, momentum, energy, and mass are specified as follows:

$$\frac{\partial u}{\partial x} + \frac{\partial v}{\partial y} = 0, \tag{5}$$

$$\frac{\partial u}{\partial t} + u \frac{\partial u}{\partial x} + v \frac{\partial u}{\partial y} = \nu \frac{\partial^2 u}{\partial y^2} + \sqrt{2} \nu \Gamma \frac{\partial u}{\partial y} \frac{\partial^2 u}{\partial y^2} - \left[\frac{\sigma B_0^2}{\rho_f(1-ct)} + \frac{\nu}{K_0} \right] u, \tag{6}$$

$$\frac{\partial T}{\partial t} + u \frac{\partial T}{\partial x} + v \frac{\partial T}{\partial y} = \alpha_f \frac{\partial^2 T}{\partial y^2} + \tau \left[D_B \frac{\partial C}{\partial y} \frac{\partial T}{\partial y} + \frac{D_T}{T_\infty} \left(\frac{\partial T}{\partial y} \right)^2 \right] - \left(\frac{1}{(\rho c)_f} \frac{\partial q_r}{\partial y} \right) + \frac{\nu}{(\rho c)_f} \left(\frac{\partial u}{\partial y} \right)^2, \tag{7}$$

$$\frac{\partial C}{\partial t} + u \frac{\partial C}{\partial x} + v \frac{\partial C}{\partial y} = D_B \frac{\partial^2 C}{\partial y^2} + \frac{D_T}{T_\infty} \frac{\partial^2 T}{\partial y^2} - K_r (C - C_\infty). \tag{8}$$

The corresponding boundary conditions are given as follows.

At \$y = 0\$,

$$u = U_w(x, t) = \frac{\alpha x}{1-ct}, \quad v = V_w(x, t) = -\frac{V_0}{\sqrt{1-ct}}, \quad T = T_w(x, t) = T_\infty + \frac{T_0 U_w x}{\nu \sqrt{1-ct}} \\ C = C_w(x, t) = C_\infty + \frac{C_0 U_w x}{\nu \sqrt{1-ct}} \tag{9}$$

and as \$y \to \infty\$,

$$u \to 0, \quad T \to T_\infty, \quad C \to C_\infty. \tag{10}$$

Using the Rosseland approximation for radiation, the radioactive heat flux is simplified as

$$q_r = -\frac{4\sigma^* \partial T^4}{3k^* y}, \tag{11}$$

where σ^* and k^* are Stezan Boltzman constant and mean absorption, respectively. By using Taylor's series, we expand T^4 about free stream temprature T_∞ and neglecting higher order term and obtain the following approximation.

$$T^4 \cong 4T_\infty^3 T - 3T_\infty^4. \tag{12}$$

Using Eqns. (11) and (12), we have

$$\frac{\partial q_r}{\partial y} \cong -\frac{16T_\infty^3 \sigma^* \partial^2 T}{3k^* \partial y^2}. \tag{13}$$

Using Eq. (13), the energy Eq. (7) takes the form

$$\begin{aligned} \frac{\partial T}{\partial t} + u \frac{\partial T}{\partial x} + v \frac{\partial T}{\partial y} = \alpha_f \frac{\partial^2 T}{\partial y^2} + \tau \left[D_B \frac{\partial C}{\partial y} \frac{\partial T}{\partial y} + \frac{D_T}{T_\infty} \left(\frac{\partial T}{\partial y} \right)^2 \right] \\ + \left(\frac{16T_\infty^3 \sigma^* \partial^2 T}{3k^* (\rho c)_f \partial y^2} \right) + \frac{v}{(\rho c)_f} \left(\frac{\partial u}{\partial y} \right)^2 \end{aligned} \tag{14}$$

The governing equations can be reduced to ordinary differential equations, using the following similarity transformations:

$$\begin{aligned} \eta = y \sqrt{\frac{U_w}{\nu x}}, \psi(x, y, t) = \sqrt{U_w \nu x} f(\eta), \\ \theta(\eta) = \frac{T - T_\infty}{T_w - T_\infty}, \varphi(\eta) = \frac{C - C_\infty}{C_w - C_\infty} \end{aligned} \tag{15}$$

where η is the dimensionless similarity variable; $f(\eta)$ is the dimensionless stream function; and $\theta(\eta)$ and $\varphi(\eta)$ are the dimensionless temperature and nanoparticles volume fraction, respectively. The stream function ψ is defined such that $u = \frac{\partial \psi}{\partial y}$ and $v = -\frac{\partial \psi}{\partial x}$. With the help of above transformations, Equation (5) is identically satisfied, and Equations (6), (7) and (8) along with boundary conditions (9) take the following forms:

$$(1 + Wef''')f''' + ff'' - f'^2 - A\left(f' + \frac{\eta}{2}f''\right) - (M^2 + K_p)f' = 0 \tag{16}$$

$$\frac{1}{Pr} \left(1 + \frac{4}{3}Rd \right) \theta'' + f\theta' - 2f'\theta - \frac{A}{2}(3\theta + \eta\theta') + Nb\theta'\varphi' + Nt(\theta')^2 + Ec f'^2 = 0 \tag{17}$$

$$\varphi'' + \frac{Nt}{Nb}\theta'' + Sc(f\varphi' - 2f'\varphi - \frac{A}{2}(3\varphi + \eta\varphi') - \gamma\varphi) = 0 \tag{18}$$

where f , θ and φ are functions of η and prime denotes derivatives with respect to η . The corresponding boundary conditions will take the following form:

$$\begin{aligned} f(0) = s, f'(0) = 1, \theta(0) = 1, \varphi(0) = 1 \\ f'(\infty) = 0, \theta(\infty) = 0, \varphi(\infty) = 0, \end{aligned} \tag{19}$$

where We is the Weissenberg number representing the Williamson number, unsteadiness parameter A , the magnetic parameter M , the porosity parameter K_p , the thermal radiation parameter Rd , the Prandtl number Pr , the Brownian parameter Nb , the thermophoresis parameter Nt , the Schmidt number Sc , the chemical reaction parameter γ (with $\gamma > 0$ and $\gamma < 0$) denoting destructive and generating chemical reaction rates, respectively), Eckert number Ec and suction (for $s < 0$) or injection (for $s > 0$) parameter s are defined as follows:

$$\begin{aligned}
 We &= \Gamma x \sqrt{\frac{2a^3}{v(1-ct)^3}}, \quad A = c/a \\
 M &= \sqrt{\frac{\sigma B_0^2}{a\rho_f}}, \quad K_p = vx/(U_w K_0) \\
 Pr &= v/\alpha_m, \quad Nb = \frac{\tau D_B (C_w - C_\infty)}{v} \\
 Nt &= \frac{\tau D_T (T_w - T_\infty)}{v T_\infty}, \quad Sc = v/D_B \\
 \gamma &= \frac{K_r x}{U_w}, \quad Ec = \frac{U_w^2}{\rho_f (T_w - T_\infty)} \\
 s &= \frac{V_0}{\sqrt{av}}, \quad Rd = \frac{4\sigma^* T_\infty^3}{kk^*}
 \end{aligned} \tag{20}$$

From engineering point of view, it is useful to examine the impacts of skin friction coefficient C_f , local Nusselt number Nu_x and Sherwood number Sh_x on the boundary layer profiles of velocity, temperature, and concentration, respectively.

Nusselt number, Sherwood number and the skin friction coefficients are, respectively, expressed as:

$$Nu_x = \frac{xq_w}{k(T_w - T_\infty)}, \quad Sh_x = \frac{xJ_w}{D_B(C_w - C_\infty)} \quad \text{and} \quad C_f = \frac{\tau_w}{1/2\rho_f U_w^2} \tag{21}$$

where, τ_w is the shear stress along the stretching surface, q_w is the heat flux from the stretching surface and J_w is the wall mass flux, are given as:

$$\tau_w = -\mu_0 \left[\frac{\partial u}{\partial y} + \frac{\Gamma}{\sqrt{2}} \left(\frac{\partial u}{\partial y} \right)^2 \right]_{y=0}, \quad q_w = -\left(k + \frac{16T_\infty^3 \sigma^*}{3k^*} \right) \left[\frac{\partial T}{\partial y} \right]_{y=0}, \quad J_w = -D_B \left[\frac{\partial C}{\partial y} \right]_{y=0} \tag{22}$$

Using the dimensionless variables, we get

$$\begin{aligned}
 \frac{-1}{2} c_f Re_x^{1/2} &= f''(0) + \frac{we}{2} f'^2(0), \\
 Nu_x Re_x^{-1/2} &= -(1 + \frac{4}{3} Rd) \theta'(0) \\
 Sh_x Re_x^{-1/2} &= -\phi'(0)
 \end{aligned} \tag{23}$$

Where, $Re_x = \frac{ax^2}{v(1-ct)}$ is the local Reynolds number.

3. Method of Solution

The physical model of ODEs alongside the boundary conditions is quantitatively evaluated by the shooting method and is implemented in MATLAB. The shooting approach involves two stages: converting the boundary value problem (BVP) into an initial value problem (IVP) and the higher-order ODEs are reduced into a system of first-order ODEs. The Newton–Raphson approach is employed in locating roots. The Runge–Kutta method of

order four is implemented in determining the solution of the IVP. The system of first-order ODEs reads as follows:

$$\left. \begin{aligned}
 y'_1 &= y_2 \\
 y'_2 &= y_3 \\
 y'_3 &= \frac{y_2^2 - y_1 y_3 + A(y_2 + 0.5 \eta y_3) + (M^2 + K_p) y_2}{1 + W_e y_3} \\
 y'_4 &= y_5 \\
 y'_5 &= \frac{-Pr[y_1 y_5 - 2y_2 y_4 - 0.5A(3y_4 + \eta y_5) + Nb y_5 y_7 + Nt y_5^2 + Ec y_3^2]}{\left(1 + \frac{4}{3} Rd\right)} \\
 y'_6 &= y_7 \\
 y'_7 &= -\frac{Nt}{Nb} y'_5 - Sc[y_1 y_7 - 2y_2 y_6 - 0.5A(3y_6 + \eta y_7) - \gamma y_6]
 \end{aligned} \right\} \tag{24}$$

where $y_1 = f, y_2 = f', y_3 = f'', y_4 = \theta, y_5 = \theta', y_6 = \varphi,$ and $y_7 = \varphi'$.

The boundary conditions become

$$\begin{aligned}
 y_1(0) &= s, y_2(0) = 1, y_4(0) = 1, y_6(0) = 1 \\
 y_2(\infty) &= 0, y_4(\infty) = 0, y_6(\infty) = 0.
 \end{aligned} \tag{25}$$

Then the IVP is solved by appropriately guessing the missing initial values of $y_3(0), y_5(0),$ and $y_7(0)$ which are not specified at initial position using the shooting method for several sets of parameters. In principle, a trial and error-method can be used to determine these initial values, but it is tedious. After solving the reduced equations (16-18) together with the boundary conditions (19) numerically using the above mentioned Runge-Kutta method for different values of flow parameters, the effects of those emerging flow parameters on the dimensionless velocity, temperature, concentration, skin-friction coefficient, the rate of heat and mass transfer are investigated. In this study, it has been considered the iterative process, which is terminated to converge when the difference between two successive values are reached 10^{-7} .

4. Results and Discussion

To have clear insight into the behavior of the fluid flow, a computational analysis has been carried out for the dimensionless velocity, heat and mass transfer profiles across the boundary layer and the results are presented in Figs. 1–14 and in Table 2. The comparison of skin friction coefficients, $-f''(0)$ between the results obtained by Kahan et al. (2017), Bibi et.al (2018) and Tesfaye et al. (2020) are shown in Table1. All results obtained by these researches are in excellent agreement with the present results. The effects of different flow parameters on the velocity, temperature and concentration distributions as well as on reduced skin friction, rate of heat and mass transfer coefficients are discussed numerically.

Table 1: Comparison of the values of $-f''(0)$ for $We = M = K_p = R_d = S_c = s = \gamma = 0, Pr = 0.72, N_b = 0.2, N_t = 0.1$ against some values of A

A	Kahan and Azm(2017)	Bibi et.al(2018)	Tesfaye et al.(2020)	Present study
0.0	1.000	1.0005	1.0000	1.0002
0.2	1.06801	1.0685	1.06874	1.0682
0.4	1.13469	1.1349	1.13521	1.13475
0.6	1.19912	1.1992	1.199930	1.19913
0.8	1.26104	-	1.26099	1.26106
1.2	1.37772	-	1.377755	1.37774
2.0	1.58737	-	1.58740	1.58738

Table 2: The values of Skin-friction coefficient, Reduced Nusselt number and Sherwood number, for different values of the flow parameters

s	A	We	M	K_p	γ	$-\frac{1}{2} c_f Re_x^{\frac{1}{2}}$	$-Nu_x Re_x^{-1/2}$	$-Sh_x Re_x^{-\frac{1}{2}}$
0.3	0.3	0.1	0.2	1.0		1.927472	1.3915792	0.402824
0.5						2.086177	1.474385	0.377508
0.7						2.259326	1.563916	0.348774
1.0						2.547191	1.710371	0.3000433
-0.5						1.420038	1.126190	0.482275
-0.2						1.588284	1.213441	0.451114
-0.1						1.649974	1.246009	0.443571
	0.0					1.830445	1.206779	0.3233211
	0.5					1.991487	1.495358	0.4460862
	1.0					2.148779	1.7163608	0.534914
		0.0				1.658188	1.411248	0.401096
		0.2				2.313762	1.367064	0.408989
		0.3				3.045867	1.326056	0.418212
			0.7			2.123112	1.348431	0.407203
			1.0			2.331808	1.304663	0.412498
			1.5			2.803796	1.218999	0.449430
				2.0		2.347697	1.302322	0.417515
				3.0		2.727533	1.232695	0.446022
				4.0		3.082498	1.171515	0.462549
					0.4	1.927472	1.1569044	0.5687456
					1.0	1.927472	0.8917168	0.7485293
					2.0	1.927472	0.673396	0.889268
					-0.1	1.927472	1.397668	0.216229
					-0.2	1.927472	1.400464	0.137439
					-0.3	1.927472	1.403976	0.043529

In Table 2, we can see that the reduced skin friction coefficient $-\frac{1}{2} c_f Re_x^{\frac{1}{2}}$ increases with increasing values of unsteady parameter A, magnetic parameter M, Weissenberg number We , porosity parameter K_p and injection parameter s (for $s > 0$) whereas it decreases with the increasing parameter of suction parameter s (for $s < 0$). The chemical reaction parameter γ (for both $\gamma < 0$ and $\gamma > 0$) doesn't have significant influence on the skin friction coefficient as it can be seen in the table. Table 2 also reveals that an increase in magnetic parameter, porosity parameter as well as Williamson parameter leads to enhance the reduced Sherwood number $-Sh_x Re_x^{-\frac{1}{2}}$ whereas the reduced Nusselt number $-Nu_x Re_x^{-1/2}$ gets depleted at the surface. The reduced coefficient of Nusselt number is increased whenever, the unsteadiness parameter, the injection parameter or the generating chemical reaction parameter increases whereas the opposite phenomena is observed for the increment of suction or destructive parameter. A rise in injection parameter or destructive parameter results a decline of reduced coefficient of Sherwood number whereas an increase in injection or generative parameter results in a rise of reduced coefficient of Sherwood numbers as it is noted in the table 2.

We see that in figures 1-3 that the velocity gradient, temperature and concentration profiles have reverse relationship with injection parameter. From these figures, it is also noted that an increase in suction parameter results in a rise of all these profiles. The result in Figure 4 shows that the temperature profiles are decreasing functions of the unsteadiness parameters in the boundary layer. Fig. 5 exhibits the effects of Weissenberg number, We on fluid flow velocity profiles. Physically, Williamson parameter is the ratio between relaxation and retardation time. The enhancing relaxation is responsible for particles of fluid to recapture their physical position. This results in increasing the fluid viscosity and thus reducing the velocity of the fluid.

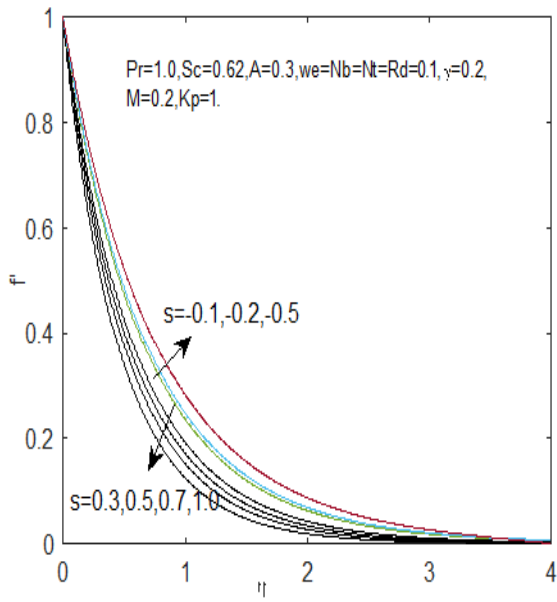


Fig. 1: Effect of suction/injection parameter s on velocity profiles

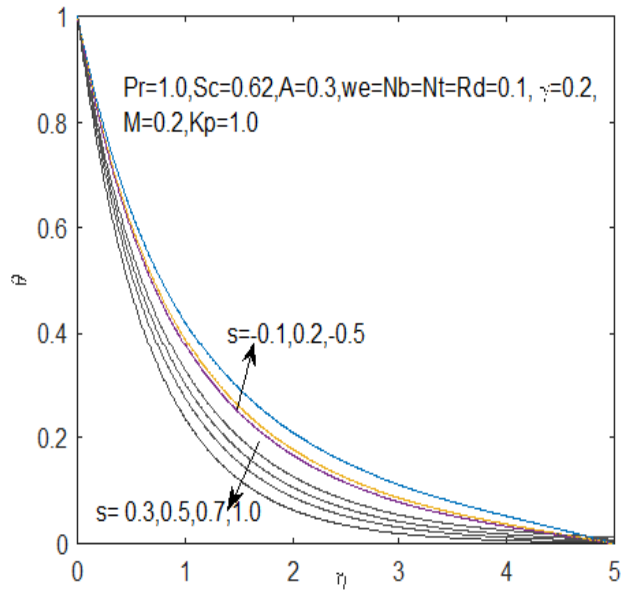


Fig. 2: Effect of suction/injection parameter s on temperature profiles

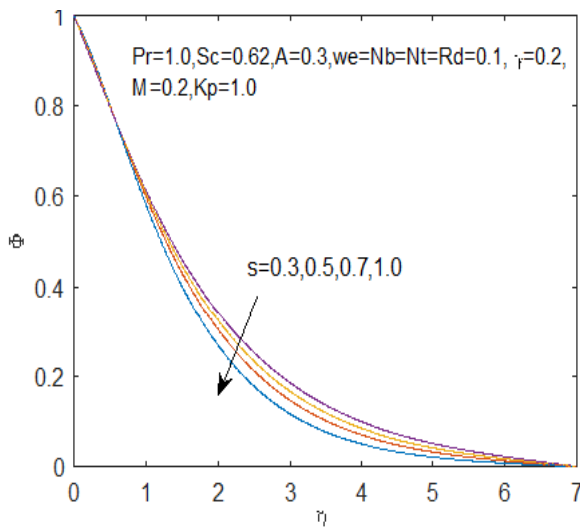


Fig. 3: Effect of suction/injection parameter s on concentration profiles

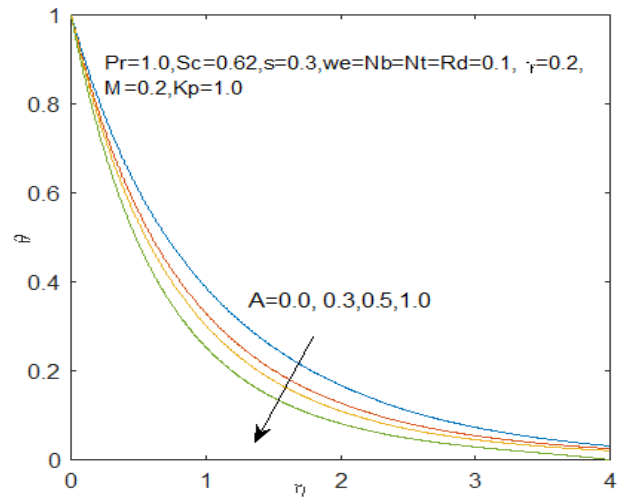


Fig. 4: Effect of suction/injection parameter A on temperature profiles

Figs. 6 and 7 depict the effects of magnetic parameter M , on dimensionless velocity and temperature distributions, respectively. The presence of a magnetic field in an electrically conducting fluid induces a force called Lorentz force, which opposes the flow. This resistive force tends to slow down the flow, so the effect of increase in M is to decrease the velocity and also causes to increase its temperature. Figs. 8 and 9 illustrate effects of the porosity parameter on velocity and temperature profiles. Obviously, the presence of porous medium causes higher restriction to the fluid flow which, in turn, slows its motion. Therefore, with an increased porosity parameter, the resistance to the fluid motion increases, and hence, velocity decreases and enhances the temperature.

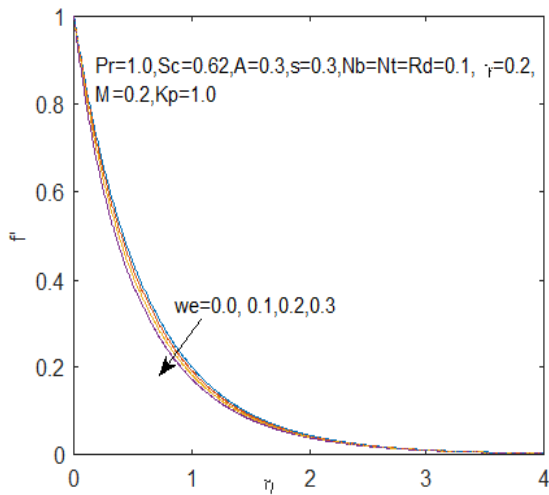


Fig. 5: Effect of Weissenberg number on velocity profiles

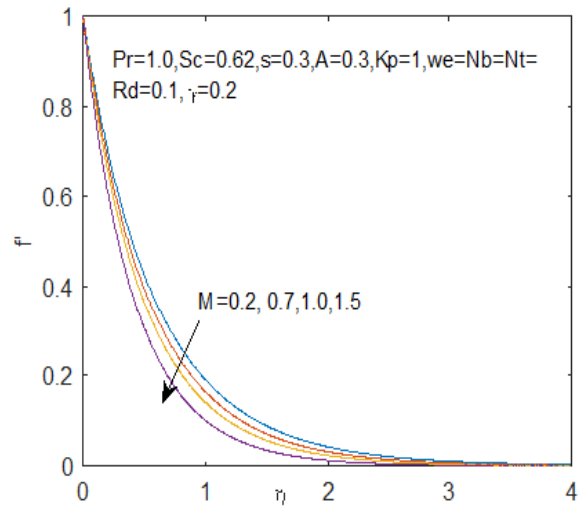


Fig. 6: Effect of magnetic parameter M on velocity profiles

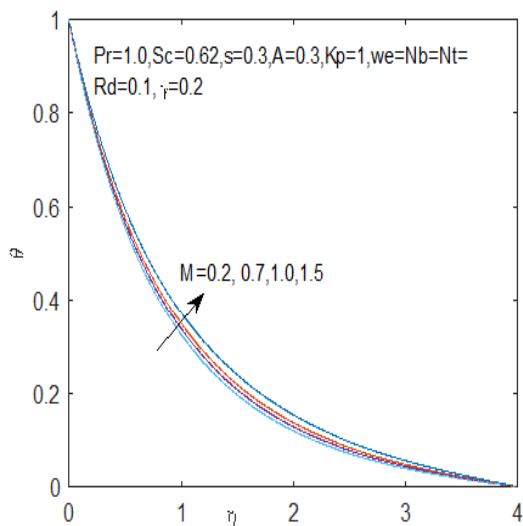


Fig. 7: Effect of magnetic parameter M on temperature profiles

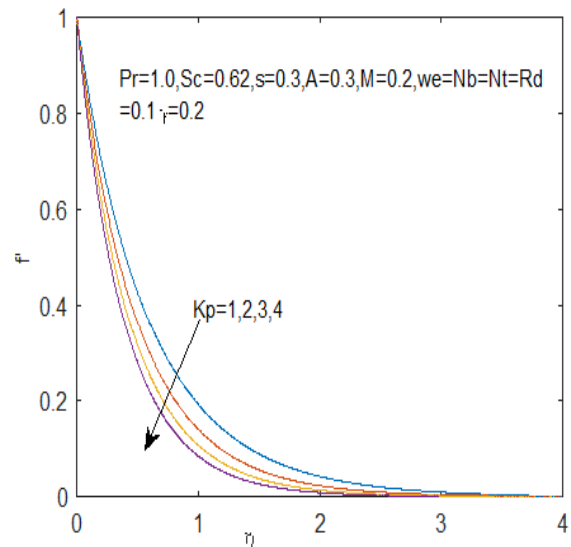


Fig. 8: Effect of porosity parameter Kp on velocity profiles

Figure 10 examines the effect of the Prandtl number Pr on the temperature profile. The increase in the Prandtl number leads to a reduction in the thermal boundary layer, thus reducing the temperature profile. The increase in the Prandtl number makes the kinematic viscosity stronger than density, which generates resistive force against the flow of the fluid. This phenomenon makes the nanofluid thicker, and thus reduction in the thermal profile is depicted. The effect of the Schmidt number (Sc) on the velocity is demonstrated in Fig.11. The Schmidt number (Sc) embodies the ratio of the momentum diffusivity to the mass (species) diffusivity. It physically relates the relative thickness of the hydrodynamic boundary layer and mass-transfer (concentration) boundary layer. In the figure, it is noticed that as Schmidt number (Sc) increases the temperature profiles decreases. Fig. 12 is drawn to examine the effects of thermal radiation parameter Rd on temperature profiles. It is noted that the temperature distribution is enhanced significantly with the increase of Rd because an increase in the radiation parameter provides more heat to fluid that causes an enhancement in the temperature and thermal boundary layer thickness.

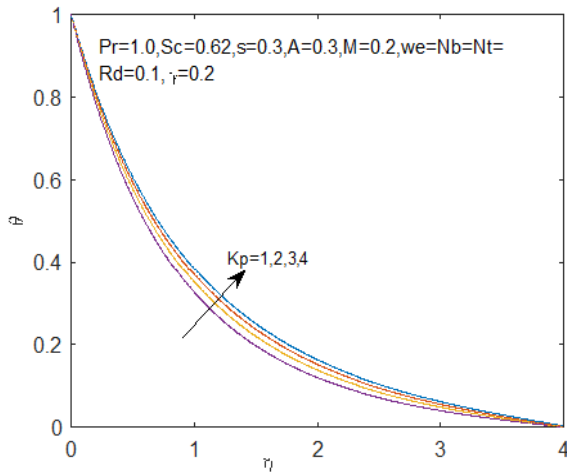


Fig. 9: Effect of porosity parameter K_p on temperature profiles

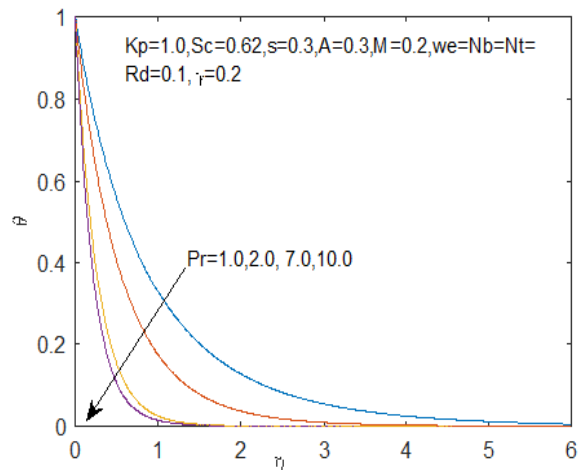


Fig. 10: Effect of Prandtl number Pr on temperature profiles

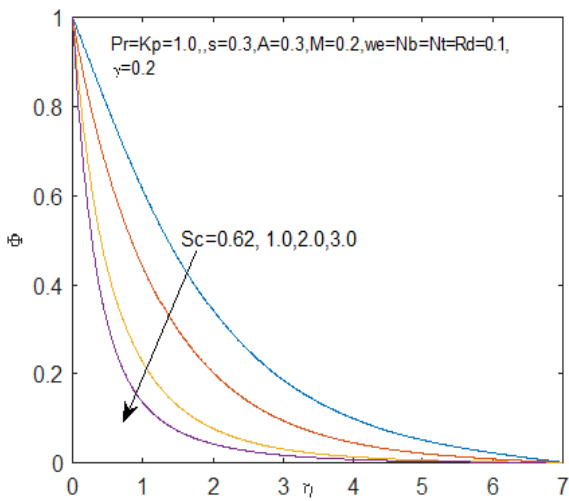


Fig. 11: Effect of Schmidt number on concentration profiles

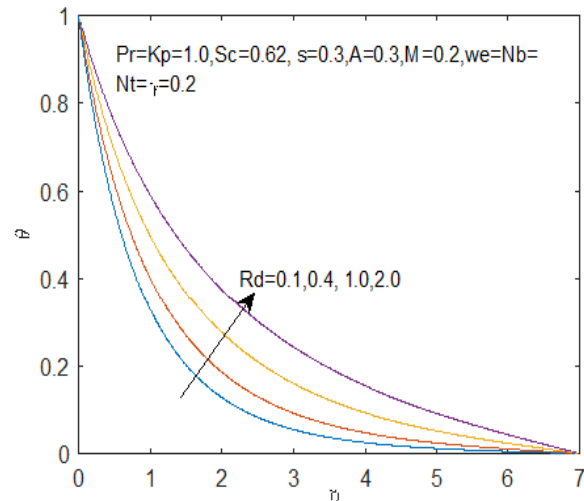


Fig. 12: Effect of thermal radiation parameter on temperature profiles

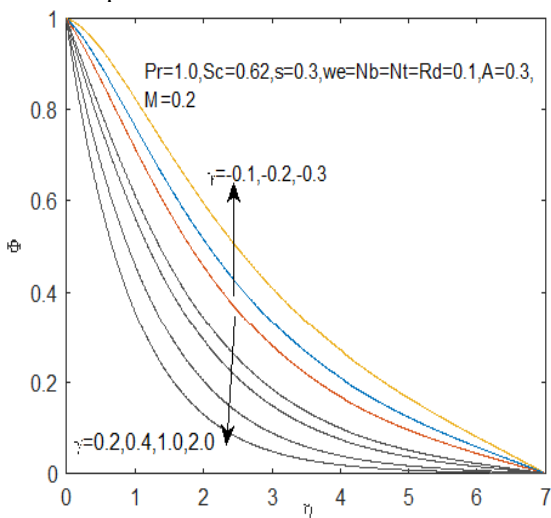


Fig. 13: Effect of chemical reaction parameter on concentration profiles

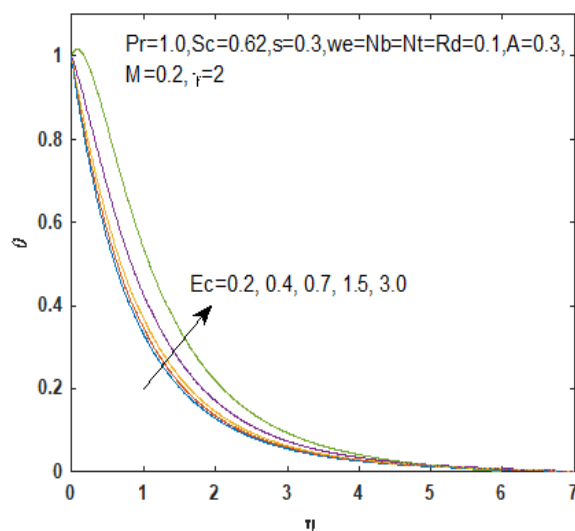


Fig. 14: Effect of Eckert number Ec on temperature profiles

The effect of chemical reaction parameter γ on concentration profile is highlighted in Fig. 13 for species consumption and generation cases. We can see here in the figure that the concentration profile decreases for the destructive chemical reaction parameter and increases for the generative chemical reaction parameter. In Figure 14, it indicates that increasing the value of Eckert number Ec has the enhancing effect on temperature profile and increases the thermal boundary layer thickness in the flow field. The Eckert number expresses the relationship between the kinetic energy in the flow and the enthalpy. It embodies the conversion of kinetic energy into internal energy by work done against the viscous fluid stresses and generates heat in the fluid and hence increases the temperature as the Eckert number increases.

5. Conclusion

A boundary layer analysis for the unsteady flow, heat, and mass transfer of the Williamson nanofluid over a heated permeable stretching sheet embedded in porous medium in the presence of viscous dissipation is presented. The governing equations are approximated to a system of non-linear ordinary differential equations by similarity transformation and solved numerically using fourth order Runge-Kutta method along shooting technique. Numerical calculations are carried out for various values of the dimensionless parameters of the problem. The results are presented graphically and in a table. The primary outcomes of the problem are summarized as follows:

- A rise in injection parameter or destructive parameter results a decline of reduced coefficient of Sherwood number whereas an increase in injection or generative parameter results in a rise of reduced coefficient of Sherwood numbers.
- By increasing values of injection parameter, the decrease of the velocity, temperature or concentration profiles is found.
- Increasing values of suction parameters results in increasing values of both the velocity and the temperature profile.
- Increasing magnetic parameter decreases the velocity profile whereas it increases the temperatures profiles.
- Chemical reaction parameter decreases the concentration profile whereas the velocity and temperature of the fluid are not significantly changed with increasing values of chemical reaction parameter.
- Velocity profile decrease and temperature profile increases for increasing values of the porosity parameter.
- A decrease in velocity profile of the fluid is observed for increasing values of the Williamson parameter.
- The effect of Eckert number is to increase the temperature of the fluid in the boundary layer.
- It is noted that the temperature distribution is enhanced significantly with the increase of thermal radiation parameter.
- The increase in the Prandtl number leads to a reduction in the thermal boundary layer, and thus reducing the temperature profile.

Acknowledgements

The author is grateful and expresses sincere thanks to the reviewers for their detailed reading, precious proposals, and comments.

References

- Sakiadis, B.C.(1961): Boundary-layer behavior on continuous solid surfaces: I. Boundary-layer equations for two-dimensional and axisymmetric flow, AICHE Journal, vol. 7, no. 1, pp. 26-28. <https://doi.org/10.1002/aic.690070108>.
- Crane, L.J. (1970): Flow past a stretching plate, Z. Angew. Math. Phys., Vol.21, pp. 645-647. <https://doi.org/10.1007/BF01587695>
- Gupta, P.S. and Gupta, A.S. (1977): Heat and mass transfer on stretching sheet with suction or blowing, Can. J. Chem. Eng., Vol. 55, pp.744-746, <https://doi.org/10.1002/cjce.5450550619>
- Pop, I. and Na, T.Y. (1996): Unsteady flow past a stretching sheet. Mech. Res. Commun., Vol.23, pp.413-422. [https://doi.org/10.1016/0093-6413\(96\)00040-7](https://doi.org/10.1016/0093-6413(96)00040-7)
- Kumar, R. (2013): MHD boundary layer flow on heat and mass transfer over a stretching sheet with slip effect, Journal of Naval Architecture and Marine Engineering, vol. 10, no. 2, pp. 109-118. <https://doi.org/10.3329/jname.v10i2.16400>
- Kumar,N.S. Kumar,R. and Vijaya Kumar,A.G.(2016.): thermal diffusion and chemical reaction effects on unsteady flow past a vertical porous plate with heat source dependent in slip flow regime, Journal of Naval Architecture and Marine Engineering, vol. 13, no. 1, pp. 51-62. <https://doi.org/10.3329/jname.v13i1.20773>
- Williamson, R.V.(1929): The flow of pseudo plastic materials, Ind. Eng. Ch., vol. 21, no. 11, pp. 1108-1111. <https://doi.org/10.1021/ie50239a035>
- Dapra, I. and G. Scarpi, G. (2007): Perturbation solution for pulsatile flow of a non-Newtonian Williamson fluid in a rock fracture, Int. J. Rock Mech. Min. Sci. Vol. 44, pp. 271-278. <https://doi.org/10.1016/j.ijrmmms.2006.07.003>
- Vasudev, C., Rao, U.R., Reddy, M.V.S.and Rao, G.P. (2010): Peristaltic Pumping of Williamson fluid through a porous medium in a horizontal channel with heat transfer, Amer. J. Sci. Ind. Res., Vol.1, Nn.3,pp. 656-666. <https://doi.org/10.5251/ajsir.2010.1.3.656.666>
- Nadeem, S. and Akbar, N.S.(2010): Numerical solutions of peristaltic flow of Williamson fluid with radially varying MHD in an endoscope, Internat. J Numer. Methods Fluids, Vol. 66, pp. 212-220. <https://doi.org/10.1002/flid.2253>
- Nadeem, S. and Hussain, S.T. (2014): Flow and heat transfer analysis of Williamson nanofluid, Appl. Nanosci., Vol. 4, pp.1005-1012. <https://doi.org/10.1007/s13204-013-0282-1>
- Nadeem, S. and Hussain, S.T(2016): Analysis of MHD Williamson nano fluid flow over a heated surface, J. Appl. Fluid Mech.,Vol. 9 ,pp.729-739. <https://doi.org/10.18869/acadpub.jafm.68.225.21487>
- Kumaran, V. and Ramanaiah, G.(1996): A note on the flow over a stretching sheet, Acta Mecca, vol. 116, no. 1, pp. 229-233. <https://doi.org/10.1007/BF01171433>
- Gossaye, A. and Naikoti,K.(2019): Optimal Homotopy Asymptotic solution for cross-Diffusion on slip flow and heat transfer of electrical MHD Non-Newtonian fluid over a slendeing stretching sheet, Int. Journal of Applied and Computational mathematics, Vol. 5,no.3. <https://doi.org/10.1007/s40819-019-0679-y>
- Gossaye, A. (2020): Analytic Treatment for Electrical MHD Non-Newtonian Fluid Flow over a stretching Sheet through a Porous Medium, Advances in Mathematical Physics, Volume 2020, Article ID 8879264, 14 pages, <https://doi.org/10.1155/2020/8879264>
- Kho, Y. B., Hussanan A., Mohamed, M. K. A, Sarif, N. M., Ismail, Z. and Salleh, M Z (2017): Thermal radiation effect on MHD flow and heat transfer analysis of Williamson nanofluid past over a stretching sheet with constant wall temperature, Journal of Physics: Conference Series 890012034. <https://doi.org/10.1088/1742-6596/890/1/012034>
- Khan M., Malik ,M.Y., Salahuddin, T. and Hussian, A.(2018): Heat and mass transfer of Williamson nanofluid flow yield by an inclined Lorentz force over a nonlinear stretching sheet Results in Physics,Vol. 8,pp. 862-868. <https://doi.org/10.1016/j.rinp.2018.01.005>
- Mabood F., Ibrahim, S. M., Lorenzini. G. and Lorenzini,E.(2017): Radiation effects on Williamson nanofluid flow over a heated surface with magnetohydrodynamics, International Journal of Heat and Technology,Vol. 35,no.1,pp. 196-204 .<https://doi.org/10.18280/ijht.350126>

- Vijayalaxmi, T. and Shankar, B. (2016): Hydromagnetic flow and heat transfer of Williamson nanofluid over an inclined exponential stretching sheet in the presence of thermal radiation and chemical reaction with slip conditions, *Journal of Nanofluids*, Vol. 5, no.6, pp. 826-838. <https://doi.org/10.1166/jon.2016.1283>
- Goud, B.S., Reddy, Y.D., Rao, V.S., and Khan, Z.H. (2020): Thermal radiation and Joule heating effects on a magnetohydrodynamic Casson nanofluid flow in the presence of chemical reaction through a non-linear inclined porous stretching sheet, *J. Naval Architecture and Marine Eng.*, Vol.17, pp.143- 164, <https://doi.org/10.3329/jname.v17i2.49978>.
- Choi, S.U.S. and Eastman, J. (1995): Enhancing thermal conductivity of fluids with nanoparticle, *Master sci.*, Vol. 231, Vol. 99-105.
- Bilal Ashraf, M., Hayat, T., Alsaedi, A., and Shehzad, S. A. (2015): Convective heat and mass transfer in MHD mixed convection flow of Jeffrey nanofluid over a radially stretching surface with thermal radiation, *J. Cent. South Univ.*, Vol. 22, no.3, pp.1114-1123, <https://doi.org/10.1007/s11771-015-2623-6>
- Shehzad, S. A., Hussain, T., Hayat, T., Ramzan, M., and Alsaedi, A. (2015): Boundary layer flow of third grade nano fluid with Newtonian heating and viscous dissipation, *J. Cent. South Univ.*, Vol. 22, no.1, pp. 360-367. <https://doi.org/10.1007/s11771-015-2530-x>
- Madhu, M., and Kishan, N. (2015): Magnetohydrodynamic mixed convection stagnation-point flow of a power-law non-Newtonian nanofluid towards a stretching surface with radiation and heat source/sink, *J. Fluids*, Vol. 14. <https://doi.org/10.1155/2015/634186>
- Krishnamurthy, M.R., Prasannakumara, B.C., Giressha, B.J. and R. S. R. Gorla, R.S.R. (2016): Effect of chemical reaction on MHD boundary layer flow and melting heat transfer of Williamson nanofluid in porous medium, *Engineering Science and Technology, an International Journal*, vol. 19, no. 1, pp. 53-61. <https://doi.org/10.1016/j.jestch.2015.06.010>
- Kho, Y.B., Hussanan, A., Mohamed, M.K.A., Sarif, Z., Ismail, N.M., and M. Z. Salleh, M.Z. (2017): thermal radiation effect on MHD flow and heat transfer analysis of Williamson nanofluid past over a stretching sheet with constant wall temperature, *Journal of Physics: Conference Series*, vol. 890, Article ID012034. <https://doi.org/10.1088/1742-6596/890/1/012034>
- Shawky, H.M., Eldabe, N.T.M., Kamel, K.A. and Abd-Aziz, E.A. (2019): MHD Flow with Heat and Mass Transfer of Williamson Nanofluid over Stretching Sheet through Porous Medium, *Microsyst Technol*, Vol. 25, pp.1155-1169. <https://doi.org/10.1007/s00542-018-4081-1>
- Tesfaye, K., Eshetu, H. and Tadesse, W. (2020): Heat and mass transfer in unsteady boundary layer flow of Williamson Nanofluids, *Journal of Applied Mathematics*, V.2020, Article ID1890972, 13 pages. <https://doi.org/10.1155/2020/1890972>
- Manjula, N., Govardhan, K., M. N. Rajashekar, M.N. (2019): Effect of Viscous Dissipation on MHD Williamson Nanofluid Flow in a Porous Medium, *International Journal of Recent Technology and Engineering (IJRTE)* ISSN: 2277-3878, Vol.8 no.3. <https://doi.org/10.35940/ijrte.C4861.098319>
- Wubshet, I. and Mekonnen, N. (2020): The Investigation of MHD Williamson Nanofluid over Stretching Cylinder with the Effect of Activation Energy. *Advances in Mathematical Physics* Volume 2020, Article ID 9523630, 16 pages. <https://doi.org/10.1155/2020/9523630>
- Nadeem, S., and Hussain, S. T. (2013): Flow and heat transfer analysis of Williamson nanofluid, *Appl. Nanosci.*, Vol. 4, no.8, pp. 1005-1012. <https://doi.org/10.1007/s13204-013-0282-1>
- Dapra, I., and Scarpi, G. (2007): Perturbation solution for pulsatile flow of a non-Newtonian Williamson fluid in a rock fracture, *Int. J. Rock Mech. Min. Sci.*, Vol.44, no.2, pp. 271-278. <https://doi.org/10.1016/j.ijrmms.2006.07.003>
- Khan, M. and Azam, M. (2017): Unsteady heat and mass transfer mechanisms in MHD Carreau nan fluid flow, *Journal of Molecular Liquids*, vol. 225, pp. 554-562. <https://doi.org/10.1016/j.molliq.2016.11.107>
- Bibi, M., Rehman, K.U., Malik, M.Y., and Tahir, M. (2018): Numerical study of unsteady Williamson fluid flow and heat transfer in the presence of MHD through a permeable stretching surface, *European Physical Journal Plus*, vol. 133, no. 4, pp.154. <https://doi.org/10.1140/epjp/i2018-11991-2>